Effect of Voltage Drop within the Synaptic Cleft on the Current and Voltage Generated at a Single Synapse

Leonid P. Savtchenko,*† Sergey N. Antropov,† and Sergey M. Korogod*†
*Unite de Neurocybernetique cellulaire, CNRS/UPR 9041, 13009 Marseille, France, and †Laboratory of Biophysics and Bioelectronics, Dniepropetrovsk State University, 320625 Dniepropetrovsk, Ukraine

ABSTRACT In a model of a single synapse with a circular contact zone and a single concentric zone containing receptor-gated channels, we studied the dependence of the synaptic current on the synaptic cleft width and on the relative size of the receptor zone. During synaptic excitation, the extracellular current entered the cleft and flowed into the postsynaptic cell through receptor channels distributed homogeneously over the receptor zone. The membrane potential and channel currents were smaller toward the cleft center if compared to the cleft edges. This radial gradient was due to the voltage drop produced by the synaptic current on the cleft resistance. The total synaptic current conducted by the same number of open channels was sensitive to changes in the receptor zone radius and the cleft width. We conclude that synaptic geometry may affect synaptic currents by defining the volume resistor of the cleft. The in-series connection of the resistances of the intracleft medium and the receptor channels plays the role of the synaptic voltage divider. This voltage dividing effect should be taken into account when the conductance of single channels or synaptic contacts is estimated from experimental measurements of voltage-current relationships.

INTRODUCTION

Synaptic transmission is crucial for communication in the central nervous system. One of the hallmarks of synaptic transmission is its modifiability, which changes synaptic efficacy (Burns and Augustine, 1995). The dynamic organization of synaptic structure is manifested in modifications of the size and shape of synaptic elements, particularly the postsynaptic density (PSD) (Geinisman et al., 1993; Schubert, 1991). The PSD is distinguished from other parts of the contact zone as the region with the highest concentration of neurotransmitter receptors and ion channels (Kelly et al., 1984; Siekevitz, 1985; Kennedy et al., 1990), and therefore functionally it is often referred to as the receptor zone. Any biophysical concept of synaptic function operates with synaptic currents through the receptor channels condensed in the receptor zone. How do the size, the shape, and the relative location of the receptor zone influence the postsynaptic potentials and currents generated in a single synaptic contact? So far this important question has no clear answer because this level of cellular organization is not readily accessible in experiments. Previous theoretical studies were mainly focused on the consequences of the structural arrangement of the synaptic contact for diffusion and receptor binding of neurotransmitters released into the cleft (Kleinle et al., 1996; Uteshev and Pennefather, 1996; Rusakov and Kullmann, 1998a). The electric phenomena in the cleft, as opposed to mass transfer, remained practically beyond the scope of research (however, see the discussion of synaptic efficiency in Eccles and Jaeger, 1958). The aim of the present study was to elucidate the impact of the cleft geometry on the electric current generated during synaptic activation. This was considered in a simplified model of a circular synaptic contact zone containing a single, concentric active receptor zone homogeneously populated by voltage-independent receptor channels.

THEORY

Simulated single synaptic contact (including pre- and postsynaptic membranes separated by the cleft) was represented by a flat circular cylinder or disk of radius R (radius of the contact zone) and thickness δ (the cleft width) (Fig. 1). The postsynaptic base of the disk contained a concentric receptor zone of radius $r \leq R$. This representation is conventional for models (Kleinle et al., 1996). The specific resistivity of the conductive medium that fills in the cleft and the bulk of the extracellular space was R_{ex}. Excitatory synaptic current (reversal transmembrane potential $E_S = 0$ mV) entered the cleft from the bulk of the extracellular space via the side surface of the disk. The radial density of the current was homogeneous. In the cleft, the radial current decreased with radius ρ and vanished at the center ($\rho = 0$) because it flowed to the postsynaptic cell through N identical channels activated by the neurotransmitter. The channels were homogeneously distributed over the receptor zone with the density $\sigma = N/\pi gr^2$. We considered steady synaptic activation, assuming constant values of N and of the single channel conductance γ. The thickness of the cleft δ was much smaller than the thickness δ_{in} of the postsynaptic submembrane layer of cytoplasm. The current flow across the presynaptic base of the cylinder was neglected. The intracellular potential was homogeneous ($E_{in} = -65$ mV) within the contact zone, and the transmembrane voltage $E =$

Received for publication 7 July 1999 and in final form 6 November 1999.
Address reprint requests to Dr. Leonid P. Savtchenko, Unite de Neurocybernetique cellulaire, UPR/CNRS 9041, 280 Boulevard Sainte-Marguerite, 13009 Marseille, France. Tel.: 33-4-91-75-02-00; Fax: 33-4-91-26-20-38; E-mail: leon@marseille.inserm.fr.

0006-3495/00/03/1119/07 $2.00

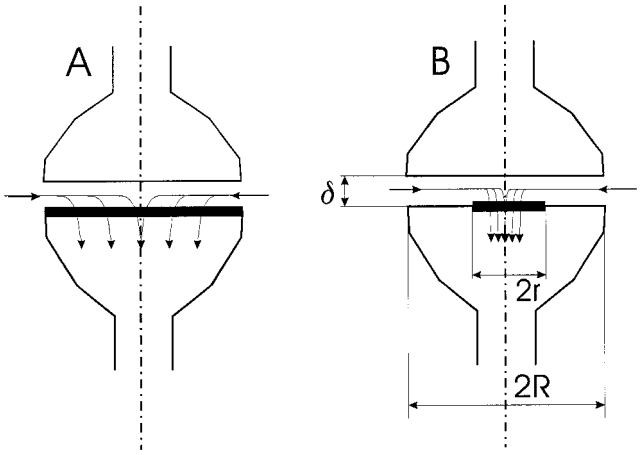

FIGURE 1 Schematic representation of simulated synaptic contact in the section perpendicular to planes of the pre- and postsynaptic membranes separated by the cleft of width δ. The contact zone was circular, with a radius $R = 1$ μm. The receptor zone was concentric with the same ($r = R$) (*A*) or smaller ($r = 0.2$ μm) (*B*) radius. In both cases, the receptor zone (*thick black line*) had $N = 200$ homogeneously distributed open receptor channels conducting synaptic current (*arrows*).

$E_{in} - E_{ex}$ was clamped at the edge of the cleft to $E(R) = E_C = -65$ mV. With these assumptions, the following forms of the cable differential equation defined the transmembrane voltage $E(\rho, t)$ within and outside the receptor zone, respectively:

$$-\frac{\partial}{\partial\rho}\left(-\frac{1}{r_{ex}}\frac{\partial E}{\partial\rho}\right) = g_s(E - E_s) + c_m\frac{\partial E}{\partial t} \quad r > \rho > 0 \qquad (1a)$$

and

$$-\frac{\partial}{\partial\rho}\left(-\frac{1}{r_{ex}}\frac{\partial E}{\partial\rho}\right) = c_m\frac{\partial E}{\partial t} \quad R > \rho > r \qquad (1b)$$

where $r_{ex} = R_{ex}/2\pi\rho\delta$ and c_m are, respectively, the intracleft resistance and the subsynaptic membrane capacitance per unit radial extent of a circular disk of radius ρ, and $g_S = \gamma\sigma 2\pi\rho$ is the conductance per unit radial extent of a ring of radius ρ in the receptor zone. Thus $i_s(\rho) = g_s(E - E_S)$ is the synaptic current through this unitary ring of the receptor zone, and $(-1/r_{ex})(dE/d\rho) = i_{ex}(\rho)$ is the radial current through the disk ring of unitary length in the cleft. In these equations, the resistance r_{in} of the submembrane cytoplasm layer was neglected because $r_{ex} \gg r_{in} = R_{in}/2\pi\rho\delta_{in}$, because $\delta \ll \delta_{in}$ and $R_{ex} = R_{in}$. The boundary conditions assumed the voltage clamp at the edge of the cleft,

$$E(R) = E_C, \quad \text{at } \rho = R \qquad (2a)$$

and vanishing of the radial current at the center of the cleft,

$$\left(-\frac{1}{r_{ex}}\frac{dE}{d\rho}\right) = i_{ex}(\rho) = 0 \quad \text{at } \rho = 0 \qquad (2b)$$

On the border $\rho = r$ of the receptor zone, the additional conditions were those of continuity of the voltage,

$$E(\rho)\big|_{\rho=r-} = E(\rho)\big|_{\rho=r+} = E(r) \qquad (2c)$$

and of conservation of the current,

$$\left(-\frac{1}{r_{ex}}\frac{dE}{d\rho}\right)\Big|_{\rho=r-} = \left(-\frac{1}{r_{ex}}\frac{dE}{d\rho}\right)\Big|_{\rho=r+} \qquad (2d)$$

Equation 1a can be rewritten in the conventional form of the equation

$$\frac{1}{r_{ex}}\frac{\partial^2 E}{\partial\rho^2} + \frac{1}{r_{ex}}\frac{1}{\rho}\frac{\partial E}{\partial\rho} - \frac{2\gamma N(t)\rho}{r^2}(E - E_s) = c_m\frac{\partial E}{\partial t} \qquad (2e)$$

The bell-shaped time course of $N(t)$ is given by the double-exponential function

$$N(t) = (\exp(-t/t_d) - \exp(-t/t_r))$$

where t_r is the rise time constant, with an order of magnitude of ~200 μs (Khanin et al., 1996), and t_d is the decay time constant, with an order of magnitude of ~1 ms. Because the time constant $\tau = C_m/g_s$ of Eq. 2e has an order of magnitude between 70 μs at $N = 20$ and 7 μs at $N = 200$, we can use the steady-state approximation to define the profile of E into the synaptic cleft when $N > 20$. Thus, introducing $\lambda^2 = 1/(r_{ex}g_s) = \delta/\gamma\sigma R_{ex}$, the last equation in the steady-state condition can be rewritten in the conventional form of the modified Bessel equation in dimensionless coordinate $P = \rho/\lambda$

$$\frac{\partial^2 E}{\partial P^2} + \frac{1}{P}\frac{\partial E}{\partial P} - (E - E_s) = 0$$

With the conditions in Eqs. 2b and 2c, this equation has the following general solution, expressed in modified zero-order Bessel functions I_0 of the first kind:

$$E(\rho) = (E(r) - E_s)I_0(\rho/\lambda)/I_0(L) + E_s, \quad r > \rho > 0, \qquad (3)$$

where $L = r/\lambda = (\gamma N R_{ex}/\pi\delta)^{1/2}$ is the dimensionless size characteristic of the receptor zone with a fixed number, N, of open channels. Equation 1b means conservation of the radial current $i_{ex}(\rho)$ in the cleft outside the receptor zone:

$$i_{ex}(\rho) = (-2\pi\delta/R_{ex})\rho(dE/d\rho) = J_{ex} = \text{const.}, \quad R > \rho > r \qquad (4)$$

Integration of Eq. 4 gives

$$E_C - E(r) = -J_{ex}(R_{ex}/2\pi\delta)\ln(R/r) \qquad (5)$$

from which the constant current can be defined as

$$J_{ex} = \frac{2\pi\delta}{R_{ex}}\frac{E(r) - E_c}{\ln(R/r)} \qquad (6)$$

On the other hand, using Eqs. 3 and 2d, J_{ex} can be expressed

as

$$J_{ex} = -\frac{2\pi\delta}{R_{ex}}\frac{LI_1(L)}{I_0(L)}(E(r) - E_s) \quad (7)$$

where $I_1(L) = dI_0(L)/dL$ and I_0 are the modified Bessel functions of the first kind, of the first and the zero order, respectively. The integral formulas for these functions are

$$I_0(x) = \frac{1}{\pi}\int_0^{\pi} e^{x\cos\theta}d\theta$$

and

$$I_1(x) = \frac{1}{\pi}\int_0^{\pi} e^{x\cos\theta}\cos(\theta)d\theta$$

(see, e.g., Abramowitz and Stegun, 1972, pp. 374–377).

By substituting Eq. 6 into Eq. 7, we obtain $E(r)$:

$$E(r) = \frac{E_c + E_s L\ln(R/r)I_1(L)/I_0(L)}{1 + L\ln(R/r)I_1(L)/I_0(L)} \quad (8)$$

Substituting Eq. 8 into Eqs. 3 and 5 ultimately gives the potential within and outside the receptor zone, respectively:

$$E(\rho) = E_s + \frac{(E_c - E_s)I_0(\rho/\lambda)/I_0(L)}{1 + L\ln(R/r)I_1(L)/I_0(L)}, \quad r > \rho > 0 \quad (9)$$

$$E(\rho) = \frac{E_c + (E_c\ln(\rho/r) + E_s\ln(R/\rho))LI_1(L)/I_0(L)}{1 + L\ln(R/r)I_1(L)/I_0(L)}, \quad R > \rho > r \quad (10)$$

Given the condition of conservation (Eq. 4), the total synaptic current J_S through the entire receptor zone equals J_{ex}. Thus it can be defined by integrating the elementary currents $i_{ex}(\rho)d\rho$ over $\rho \in [0, r]$ or by use of Eqs. 6–8. These two approaches lead to the same expression:

$$J_s = -\frac{2\pi\delta}{R_{ex}}\frac{LI_1(L)/I_0(L)}{1 + L\ln(R/r)I_1(L)/I_0(L)}(E_c - E_s) \quad (11)$$

It is worth noting that, because of the equality $L = r/\lambda = (\gamma NR_{ex}/\pi\delta)^{1/2}$, the Bessel functions I_0 and I_1 in Eq. 11 do not depend on either r or R, and J_S depends on the ratio R/r and on the factor $(E_C - E_S)$. Taking the ratio of the total currents defined by Eq. 11 for $r < R$ and $r = R$, we obtain the following characteristic of the synapse independent of E_C and E_S:

$$K = \frac{J_s(R/r)}{J_s(R/R)} = \frac{1}{1 + \ln(R/r)LI_1(L)/I_0(L)} \quad (12)$$

The ratio K depends on the geometrical parameters of the contact R, r, and δ on the resistivity R_{ex} of the extracellular medium and on the number N and conductance γ of the receptor channels.

METHODS

The numerical calculations of Eqs. 8–10 and 12 were performed using IDL (Interactive Data Language, version 5.2.1; Research System).

R_{ex} was changed from 100 Ω cm to 500 Ω cm in five steps, covering the range of resistivity given in the literature. The width of the synaptic cleft was changed from 10 nm to 20 nm in two steps. We assumed constant values of $N = 200$ and of the single-channel conductance $\gamma = 20$ pS.

RESULTS AND DISCUSSION

Our theory predicts that one critical parameter that determines the electrical field gradient in the synaptic cleft due to extracellular currents is the length constant, $\lambda = r(\delta\pi/\gamma NR_{ex})^{1/2}$. The length constant depends on the receptor zone radius r, the synaptic cleft width δ, the number of open receptor channels N, the conductivity of a single receptor channel γ, and on the resistivity of the intracleft medium R_{ex}. In our simulations, we varied R_{ex} because of difficulties in estimating its real value. Even though the specific conductivity of the extracellular medium is known, the effect of the restricted extracellular space in the cleft must be considered. The effective conductivity of the intracleft medium could be decreased in comparison to the conductivity of the extracellular fluid because of to the presence of numerous extracellular domains of the membrane macromolecules. For example, Rusakov and Kullmann (1998b) described a decreased diffusivity of neurotransmitters outside of the synaptic cleft due to viscous interaction with the cell walls containing such macromolecules. Because the values of the intracleft and extracellular resistivities are not known, we explored a range of R_{ex} values between 100 and 500 Ω cm, which correspond to the physiological limits given in the literature. For example, the extracellular resistivity was 321 ± 45 Ω cm (Ranck, 1963) or 556 ± 45 Ω cm (Li et al., 1968) in the gray matter of the cerebral cortex, 580 ± 53 Ω cm in the white matter of the cerebral cortex (Li et al., 1968), 250 Ω cm (Ranck 1966) in the rat hippocampus in vivo, and 133 Ω cm (Vigmond et al., 1997) in rat hippocampal slices. In a model of electrical interactions by electrical fields between neurons (Traub et al., 1985), this parameter was varied in a range of 25–250 Ωcm. Thus the range tested in our studies is consistent with the estimates found in the literature.

Electric potential profile within the cleft

Fig. 2, *A* and *B*, exemplifies spatial profiles of the membrane potential generated by a fixed number of channels in

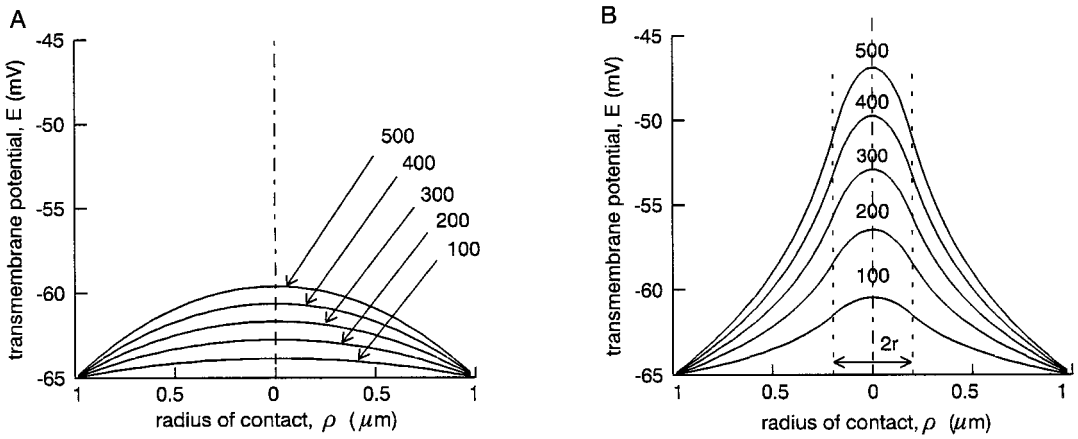

FIGURE 2 Transmembrane potential E (*ordinate*, mV) in the synaptic cleft as a function of radius ρ of the contact zone (*abscissa*, μm) for five (100–500 Ω cm) values of extracellular resistance R_{ex}. The profiles in *A* (as defined by Eq. 8) and *B* (as defined by Eqs. 9 and 10) correspond to synaptic contacts A and B, as shown in Fig. 1. Dashed lines in *B* indicate the border of the receptor zone corresponding to Fig. 1 *B*.

the synaptic contacts shown in Fig. 1, *A* and *B*, respectively, for five values of R_{ex}. The radius $R = 1$ μm and the thickness $\delta = 20$ nm of the cleft were the same, but the radii of the receptor zone were different, $r = 1$ μm (Fig. 1 *A*) and 0.2 μm (Fig. 1 *B*). In both cases, the computed membrane potential was spatially inhomogeneous within the contact zone, despite its being clamped at the cleft edge. Synaptic depolarization was greatest at the cleft center while decaying monotonically toward the edge. When the receptor zone radius r was reduced from 100% to 20% of the contact zone radius R (Fig. 1 *B*), the maximum depolarization shift at the center of the cleft was multiplied by 3.4 for each R_{ex} value (cf. Fig. 2, *A* and *B*). More than 82% of the total voltage drop occurred outside the edges of the receptor zone (Fig. 2 *B, dotted lines*). Such an inhomogeneity of the transmembrane potential $E(\rho) = E_{in} - E_{ex}(\rho)$ was due to the inhomogeneity of the extracellular potential $E_{ex}(\rho)$, inasmuch as the intracellular potential E_{in} was homogeneous over the entire contact. The extracellular potential $E_{ex}(\rho)$ was radially inhomogeneous because of the drop produced by the radial current on the intracleft resistance. An important consequence of these spatial effects was radial inhomogeneity of the synaptic driving potential that is the deviation of the inhomogeneous $E(\rho)$ from homogeneous $E_S = 0$ mV. Single channels located near the center were exposed to smaller driving potentials and thus conducted smaller currents as compared to the identical channels on the periphery of the receptor zone. The number of channels exposed to the same driving potential $(E(\rho) - E_S)$ increased with the centrifugal distance ρ: $n(\rho)d\rho = \sigma 2\pi\rho\, d\rho = (2N/r^2)\rho\, d\rho$. The total synaptic current through all $N = \int_0^R n(\rho)d\rho$ channels homogeneously distributed over the nonhomogeneously depolarized receptor zone decreased with the zonal radius r. For example, at $R_{ex} = 400$ Ω cm, the current through the small receptor zone in Fig. 1 *B* was 19.5% smaller (210 pA instead of 251 pA) than the current through the large receptor zone shown in Fig. 1 *A*. For comparison, the same population of channels would generate a 260-pA current if they all were exposed to the same driving potential of 65 mV (like those at the clamped edge of the contact). Sodium and potassium components of synaptic currents can cause significant change in the ion concentrations in the synaptic cleft. According to calculations by Attwell and Iles (1979), at the center of an activated area of radius 0.5 μm, potassium concentration increased by 2.1 mM and sodium concentration decreased by 40 mM from the initial values of $[K^+] = 2.5$ mM and $[Na^+] = 120$ mM, respectively. This produced a nonuniform distribution of equilibrium potentials for sodium and potassium ions. Therefore, the receptor channels situated near the cleft center conduct less current than peripheral ones. Consequently, the current flow through homogeneously distributed receptor channels is attenuated.

Electric field profile in the cleft: steady-state approximation

In this study we used the quasi-steady-state approximation to calculate the electric field profile within the synaptic cleft. This approximation is valid because during the opening of as few as 10 channels the time constant of the voltage relaxation within the cleft has an order of magnitude of 0.1 ms, which is smaller than the rising time constant of the synaptic current. For example, in the rat hippocampus the excitatory postsynaptic currents of the mossy fiber synapses on CA3 pyramidal cells had a mean rise time of 0.6 ± 0.1 ms (Jonas et al., 1993). When the number of open channels is small (e.g., in the beginning of the rising phase and in the end of the falling phase of the postsynaptic potential), the nonstationary equation should be used for calculation of the voltage profiles in the cleft. However, with a small number

of open channels the radial voltage gradient in the cleft is small (less than 1 mV/μm) and has little influence on the synaptic current. For that reason, the quasi-steady-state approximation is appropriate for calculation of the voltage profile in the cleft and of the synaptic current.

Total synaptic current and cleft geometry

Fig. 3 shows relative changes in the total synaptic current as a function of the receptor zone radius and the extracellular resistivity for two values of the cleft width δ, 10 nm (Fig. 3 *A*) and 20 nm (Fig. 3 *B*), as defined by Eq. 12. In the conditions of voltage clamp at the cleft edge, the total synaptic current was highest when the receptor zone represented the entire synaptic contact zone ($r = R$). Relative to this maximum value, the current decreased with smaller radii of the receptor zone at a rate that depends on the extracellular resistivity and the cleft width (compare Fig. 3, *A* and *B*). The smaller the resistivity and the thicker the cleft, the smaller were the rates and, thus, the range of the relative change in the total current for the same change in the receptor zone.

For instance, in the synapse with a $\delta = 20$-nm-wide cleft tested with five values of R_{ex} from 500 to 100 Ω cm (100 Ω cm step), the decrease in radius of the receptor zone from r = 1 μm to r = 0.2 μm reduced the total synaptic current to 200, 210, 221, 232, and 244 pA, respectively. These reductions were 24.5%, 19.5%, 14.5%, 10%, and 5.3% of the maximum values (249, 251, 253, 255, and 257 pA). In the synapse with $\delta = 10$ nm tested with the same values of R_{ex} the current was reduced by 48%, 39%, 29%, 20%, and 10%, respectively. It is noteworthy in the latter case that the maximum total currents corresponding to the same five values of R_{ex} were relatively close to each other: 249, 251, 253, 255, and 257 pA (100%, 100.8%, 101.6%, 102.4%, 103.2%), respectively.

For the different tested R_{ex}, the total currents through the receptor zone of radius $r = 0.2$ μm differed from each other less remarkably in the synapse with a wider cleft ($\delta = 20$ nm) than in that with a narrower cleft ($\delta = 10$ nm). In the first case, these currents were, respectively, 200, 210, 221, 232, and 244 pA (i.e., 100%, 105%, 110.5%, 116%, and 121%), and in the second case they were, respectively, 169, 176, 192, 209, and 231 pA (i.e., 100%, 104.1%, 113.6%, 123.6%, and 136.7%).

Plausibility of the model

The main conclusion of our study is the occurrence of a significant voltage drop produced by the synaptic current in the intracleft resistance. This also implies a significant inhomogeneity of the intracleft voltage profile. The plausibility of this phenomenon depends 1) on the relationship between the cleft width and contact zone size and 2) on the receptor channel distribution within the cleft. The cylindrical shape of the model facilitates mathematical treatment but is not critical for the phenomena in question. The cleft widths in the range of 10–20 nm used in our model were often reported for the central excitatory synapses (Peters et al., 1991; Lisman and Harris, 1993). Widening of the clefts up to 40–140 nm accompanied chromatolitic changes in the spinal motoneurons (Chen, 1978), and complete synaptic uncoupling was thought to be due to proteolitic modifications of the neuronal cell adhesion molecules by calpain present near the contact (Sheppard et al., 1991). The diameter on the order of 1 μm used for the contact zone corresponds to the values 0.69–1.47 μm derived from typical mean areas of 1.5–1.9 μm^2 of appositions (see Clements et al., 1992; Kleinle et al., 1996; and references therein). Areas of the PSDs in the range 0.02–0.26 μm^2 were described by Sorra and Harris (1993), corresponding to radii of 0.08–0.29 μm with receptor aggregates surrounded by a receptor-

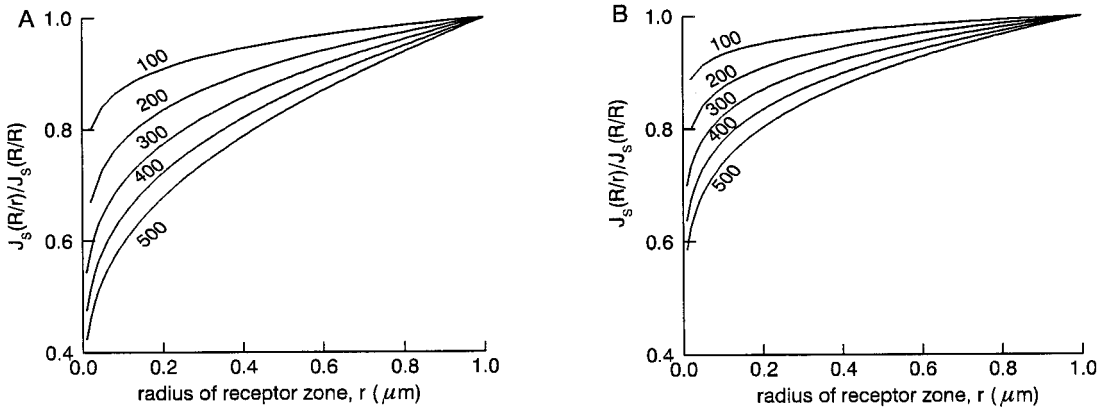

FIGURE 3 Relative change in the total synaptic current with the change in the radius *r* of the receptor zone (*abscissa*, μm) in the synapse with the contact zone of a fixed radius $R = 1$ μm for five (100–500 Ω cm) values of extracellular resistivity as defined by Eq. 12. Plots in *A* and *B* correspond to the width of the cleft $\delta = 10$ nm and $\delta = 20$ nm, respectively. Ordinates in *A* and *B*: the ratio of the total synaptic current through the receptor zone of radius *r* to the current through the receptor zone of radius $R = 1$ μm.

free zone (Faber et al., 1992, and references therein). A single-channel conductance of 20 pS corresponds to the range reported for α-amino-3-hydroxy-5-methyl-4-isoxazolepropionic acid (AMPA)-type glutamatergic receptor channels (Hille, 1992; Traynelis et al., 1993). The number of open channels ($N = 200$) during steady synaptic activation in our model is close to the upper limit of the range 10–250 given for the channels opened by single quanta of the neurotransmitter in the central synapses (Korn and Faber, 1991, and references therein). It is also consistent with the estimates obtained in freeze-fracture studies of $\sim$2800 particles/μm^2, of which some are likely to be glutamate-gated channels (Harris and Landis, 1986; Lisman and Harris, 1993). Therefore, our model keeps essential structural features of central synapses with geometrical and biophysical parameters within biologically reasonable ranges.

Mechanism of geometry-induced modulation of synaptic current

The present study highlights the causal relationship between the fine geometry of the synapse and parameters of the synaptic current. We demonstrated that the transmembrane voltage and the current through identical channels are likely to decrease toward the synaptic cleft center because of the voltage drop within the cleft. The noticeable inhomogeneity of the potentials indicates that the cleft resistance is an important determinant of the current through spatially distributed channels. The total synaptic current conducted by the same number of open channels appears to be sensitive to changes in the receptor zone radius and the cleft width. The resistive medium in the cleft plays the role of an "access" resistance for the current influx from the cleft edge toward the channels distributed in the receptor zone. This synaptic access resistance is a significant part of the effective intrinsic resistance of the synaptic current generator, electrically loaded by the extrasynaptic membrane. As follows from our derivations, the total conductance γN of open channels in the receptor zone does not give this effective resistance by simply taking the inverse value of γN.

Biological implementations

Voltage partition between the channels and the intracleft conductive medium is important for the analysis of current-voltage relations in single-synapse experiments, and characterization of the single channels is often based on such measurements (e.g., Traynelis et al., 1993). Depending on the dimensions of the contact and receptor zones and on the channel distribution, the transmembrane voltage sensed by the channels can represent only a small proportion of the total voltage drop at a synapse. This phenomenon is also important for the analysis of electric currents between synaptic and extrasynaptic parts of the membrane. Another important implementation follows from the inhomogeneity of the intracleft voltage, indicating a significant voltage gradient between inner parts and the edge of the synaptic contact. The gradients estimated from the contact dimensions and the voltages in our model ($\sim 10^4$ V/m) are sufficiently high to cause an electrophoretic drift of charged molecules within the cleft (Savtchenko et al., 1999). In the excitatory synaptic contacts, like those considered in this study, negatively charged molecules should be electrophoretically pushed out of the cleft and positively charged ones should be drawn into the cleft. These implementations are subject to our further, more detailed studies.

We are grateful to Dr. Dmitri A. Rusakov and Dr. Paul Gogan for critical reading of the manuscript.

The study was supported by the CNRS International Program for Scientific Cooperation (PICS 822).

REFERENCES

Abramowitz, M., and I. A. Stegun. 1972. Handbook of Mathematical Function, with Formulas, Graphs and Mathematical Tables, 9th printing. Dover Publications, New York.

Attwell, D., and J. F. Iles. 1979. Synaptic transmission: ion concentration changes in the synaptic cleft. *Proc. R. Soc. Lond. B.* 206:115–131.

Burns, M. E., and G. J. Augustine. 1995. Synaptic structure and function: dynamic organization yields architectural precision. *Cell.* 83:187–194.

Chen, D. H. 1978. Qualitative and quantitative study of synaptic displacement in chromatolytic spinal motoneurons of the cat. *J. Comp. Neurol.* 177:635–664.

Clements, J. D., R. A. J. Lester, G. Tong, C. E. Jahr, and G. L. Westbrook. 1992. The time course of glutamate in the synaptic cleft. *Science.* 258:1498–1501.

Eccles, J. C., and J. C. Jaeger. 1958. The relationship between the model of operation and the dimensions of the junctional regions at synapses and motor end-organs. *Proc. R. Soc. Lond. B.* 148:38–56.

Faber, D. S., W. S. Young, P. Legendre, and H. Korn. 1992. Intrinsic quantal variability due to stochastic properties of receptor-transmitter interactions. *Science.* 258:1494–1498.

Geinisman, Yu., L. de Toledo-Morrell, F. Morrell, R. E. Heller, M. Rossi, and R. F. Parshall. 1993. Structural synaptic correlate of long-term potentiation: formation of axospinous synapses with multiple, completely partitioned receptor zone. *Hippocampus.* 3:435–446.

Harris, R. M., and D. M. Landis. 1986. Membrane structure at junctions in area CA1 at the rat hippocampus. *Neuroscience.* 19:857–872

Hille, B. 1992. Ionic Channels of Excitable Membranes, 2nd Ed. Sinauer Associates, Sunderland, MA.

Jonas, P., G. Magor, and B. Sakmann. 1993. Quantal components of unitary EPSPs at the mossy fibre synapse on CA3 pyramidal cells of rat hippocampus. *J. Physiol. (Lond.).* 472:615–663.

Kelly, P. T., T. L. McGuiness, and P. Greengard. 1984. Evidence that the major PSD protein is a component of a calcium/calmodulin dependent protein kinase. *Proc. Natl. Acad. Sci. USA.* 81:945–949.

Khanin, R., L. Segel, H. Parnas, and E. Ratner. 1996. Neurotransmitter discharge and postsynaptic rise times. *Biophys. J.* 70:2030–2032.

Kennedy, M. B., M. K. Bennett, R. F. Bulleit, N. E. Erondu, V. R. Jennings, S. G. Miller, S. S. Moloy, B. L. Patton, and L. J. Schenker. 1990. Structure and regulation of type II calcium/calmodulin-dependent protein kinase in central nervous system neurons. *Cold Spring Harb. Symp. Quant. Biol.* 55:101–110.

Kleinle, J., K. Vogt, H. R. Luscher, L. Muller, W. Senn, K. Wyler, and J. Streit. 1996. Transmitter concentration profiles in the synaptic cleft: an analytical model of release and diffusion. *Biophys. J.* 71:2413–2426.

Korn, H., and D. S. Faber. 1991. Quantal analysis and synaptic efficacy in the CNS. *Trends Neurosci.* 14:439–445.

Li, C., A. F. Back, and L. Parker. 1968. Specific resistivity of cerebral cortex and white matter. *Exp. Neurol.* 20:544–557.

Lisman, J. E., and K. M. Harris. 1993. Quantal analysis and synaptic anatomy—integrating two views of hippocampal plasticity. *Trends Neurosci.* 16:141–147.

Peters, A., S. L. Palay, and H. F. Webster. 1991. The Fine Structure of the Nervous System. Neurons and Their Supporting Cells, 3rd Ed. Oxford University Press, New York and Oxford.

Ranck, J. B., Jr. 1963. Specific impedance of rabbit cerebral cortex. *Exp. Neurol.* 7:144–152.

Ranck, J. B., Jr. 1966. Electrical impedance in the subicular area of rats during paradoxial sleep. *Exp. Neurol.* 16:416–437.

Rusakov, D. A., and D. M. Kullmann. 1998a. Extrasynaptic glutamate diffusion in the hippocampus: ultrastructural constrains, uptake, and receptor activation. *J. Neurosci.* 18:3158–3170.

Rusakov, D. A., and D. M. Kullmann. 1998b. Geometric and viscous components of the tortuosity of the extracellular space in the brain. *Proc. Natl. Acad. Sci. USA.* 95:8975–8980.

Savtchenko, L. P., S. M. Korogod, and D. A. Rusakov. 1999. Electrodiffusion of synaptic receptors: a mechanism to modify synaptic efficacy 63. *Synapse.* 35:1–13.

Schubert, D. 1991. The possible role of adhesion in synaptic modification. *Trends Neurosci.* 14:127–130.

Sheppard, A., J. Wu, U. Rutishauser, and G. Lynch. 1991. Proteolytic modification of neural cell adhesion molecule (NCAM) by the intracellular proteinase calpain. *Biochim. Biophys. Acta.* 1076:156–180.

Siekevitz, P. 1985. The postsynaptic density: a possible role in long-lasting effects in the central nervous system. *Proc. Natl. Acad. Sci. USA.* 82:3494–3498.

Sorra, K. E., and K. M. Harris. 1993. Occurrence and three-dimensional structure of multiple synapses between individual radiatum axons and their target pyramidal cells in hippocampal area CA1. *J. Neurosci.* 13:3736–3748.

Traub, R. D., F. E. Dudek, C. P. Taylor, and W. D. Knowles. 1985. Simulation of hippocampal afterdischarges synchronized by electrical interactions. *Neuroscience.* 14:1033–1038.

Traynelis, S. F., R. A. Silver, and S. G. Cull-Candy. 1993. Estimated conductance of glutamate receptor channels activated during EPSCs at the cerebellar mossy fiber-granule cell synapse. *Neuron.* 11:279–289.

Uteshev, V. V., and P. S. Pennefather. 1996. A mathematical description of mPSC generation at CNS synapses. *Biophys. J.* 71:1256–1266.

Vigmond, E. J., J. L. Perez Velazquez, T. A. Valiante, B. L. Bardakjian, and P. L. Carlen. 1997. Mechanisms of electrical coupling between pyramidal cells. *J. Neurophysiol.* 78:3107–3116.